Bacillus anthracis produces membrane-derived vesicles containing biologically active toxins

Johanna Rivera[a], Radames J. B. Cordero[a], Antonio S. Nakouzi[a], Susana Frases[b], André Nicola[a,c], and Arturo Casadevall[a,d,1]

[a]Department of Microbiology and Immunology, [d]Division of Infectious Diseases, Department of Medicine, The Albert Einstein College of Medicine, Bronx, NY 10461; [b]Laboratório de Biotecnologia, Instituto Nacional de Metrologia, Normalização e Qualidade Industrial, 25 250 020, Rio de Janeiro, Brazil; and [c]Departamento de Biologia Celular, Universidade de Brasilia, 70910-900, Brasilia, Brazil

Edited by Hiroshi Nikaido, University of California, Berkeley, CA, and approved September 30, 2010 (received for review June 22, 2010)

Extracellular vesicle production is a ubiquitous process in Gram-negative bacteria, but little is known about such process in Gram-positive bacteria. We report the isolation of extracellular vesicles from the supernatants of *Bacillus anthracis,* a Gram-positive bacillus that is a powerful agent for biological warfare. *B. anthracis* vesicles formed at the outer layer of the bacterial cell had double-membrane spheres and ranged from 50 to 150 nm in diameter. Immunoelectron microscopy with mAbs to protective antigen, lethal factor, edema toxin, and anthrolysin revealed toxin components and anthrolysin in vesicles, with some vesicles containing more than one toxin component. Toxin-containing vesicles were also visualized inside *B. anthracis*-infected macrophages. ELISA and immunoblot analysis of vesicle preparations confirmed the presence of *B. anthracis* toxin components. A mAb to protective antigen protected macrophages against vesicles from an anthrolysin-deficient strain, but not against vesicles from Sterne 34F2 and Sterne δT strains, consistent with the notion that vesicles delivered both toxin and anthrolysin to host cells. Vesicles were immunogenic in BALB/c mice, which produced a robust IgM response to toxin components. Furthermore, vesicle-immunized mice lived significantly longer than controls after *B. anthracis* challenge. Our results indicate that toxin secretion in *B. anthracis* is, at least, partially vesicle-associated, thus allowing concentrated delivery of toxin components to target host cells, a mechanism that may increase toxin potency. Our observations may have important implications for the design of vaccines, for passive antibody strategies, and provide a previously unexplored system for studying secretory pathways in Gram-positive bacteria.

monoclonal antibody | passive immunity | immunizations

Anthrax is a disease caused by *Bacillus anthracis*, a Gram-positive, spore-forming, rod-like bacterium. Anthrax is primarily a disease of grazing herbivores and human cases are relatively rare, usually resulting from contact with contaminated animal products. However, *B. anthracis* has emerged as a powerful biological weapon, as illustrated by the events surrounding the delivery of bacterial spores in the mail in 2001 (1, 2). Therapy for inhalational anthrax remains unsatisfactory, as the disease has high mortality, even with the administration of potent antimicrobial agents (1). The one vaccine licensed for the prevention of anthrax is poorly immunogenic and provides only transient immunity (2).

B. anthracis owes it pathogenicity principally to two major virulence factors: a poly γ-D-glutamic acid capsule and anthrax toxins, which are encoded by two large plasmids, pXO1 and pXO2, respectively (3, 4). Three polypeptides, which act in a binary fashion, make up the anthrax toxins: protective antigen (PA), lethal factor (LF), and edema factor (EF) (3, 5). PA_{83} binds to the anthrax toxin receptor in host cells and is cleaved by a cell-associated, furin-like protease. PA_{63} polymerizes into oligomeric structures that bind EF or LF and promotes their entry into the cell (3, 5–7). Edema toxin is a calmodulin-dependent adenylate cyclase that converts intracellular ATP to cAMP, resulting in a significant increase in cAMP levels, culminating in edema (8). Lethal toxin (LeTx) is a zinc metalloprotease that cleaves cellular mitogen-activated protein kinase kinases, causing disregulation of cellular transcriptional machinery resulting in cellular death (3, 8, 9).

Secreted vesicles allow bacteria to disperse bacterial products into the surrounding environment in a concentrated manner (10, 11). Vesicle formation appears to be a conserved process among both pathogenic and nonpathogenic, Gram-negative bacteria, and the role of outer membrane vesicles in pathogenesis are of great interest. Recently, eukaryotic pathogens, such as *Cryptococcus neoformans*, have been found to release virulence factors in vesicles, suggesting that this is a widely used strategy for pathogenic microbes to deliver a noxious cargo to target immune cells (12, 13). Many Gram-negative pathogenic bacterial species, including *Pseudomonas aeruginosa*, produce vesicles that contain toxins or other virulence factors and, in several cases, vesicles have been proposed to be vehicles for toxin delivery to eukaryotic cells (14–17). Significantly less is known about the role of vesicular formation for Gram-positive bacteria. Early studies revealed the isolation of membrane-derived vesicles in Gram-positive bacteria, but these were not associated with an apparent function (18). More recently, the release of membrane-derived vesicles by Gram-positive *Staphylococcus aureus*, *Mycobacterium ulcerans*, and *Bacillus spp.* was reported (18–21), suggesting that vesicle production is a widespread phenomenon among microbial species.

The catalyst for this study was our recent serendipitous observation that immunogold studies of *B. anthracis* cells using mAbs to anthrax toxin proteins revealed clustering of gold particles in bacterial membranes and extracellular spaces (22). Such clustering implied that anthrax toxin components were concentrated in localized regions, a finding that was counterintuitive if the secretion system involved the release of single proteins from cell surfaces then diffused outwards. Given a similar experience with fungal polysaccharides of *C. neoformans*, where immunogold clustering in cell-wall micrographs led to the discovery of an extracellular vesicular transport system for polysaccharide export (12, 13), we investigated the possibility that vesicle-related phenomena were responsible for the clustering of gold particles in *B. anthracis* cellular preparations. We report that membrane-derived vesicles are produced and released by *B. anthracis* and that these vesicles contain anthrax toxin components, suggesting a physiological role for the vesicles during anthrax.

Results

Isolation of Vesicles from *B. anthracis* 34F2 Culture Supernatants. Using methods adapted from those previously developed for the study of cryptococcal vesicles (12, 13, 23), we report the presence,

Author contributions: J.R. designed research; J.R., R.J.B.C., A.S.N., S.F., and A.N. performed research; J.R., R.J.B.C., S.F., and A.N. contributed new reagents/analytic tools; J.R. and A.C. analyzed data; and J.R. wrote the paper.

The authors declare no conflict of interest.

This article is a PNAS Direct Submission.

[1]To whom correspondence should be addressed. E-mail: casadeva@aecom.yu.edu.

This article contains supporting information online at www.pnas.org/lookup/suppl/doi:10.1073/pnas.1008843107/-/DCSupplemental.

synthesis, and isolation of vesicles in *B. anthracis* Sterne culture supernatants using four techniques. First, vesicles were visualized by transmission electron microscopy, which revealed circular structures, some of which appeared to have double membranes (Fig. 1). Further analysis of vesicle dimensions by transmission electron microscopy and histogram revealed a heterogeneous population with average diameters of 50 to 300 nm (Fig. S1*A*). Second, staining of putative vesicle preparations with DiO followed by flow cytometry analysis revealed lipid-containing structures with dimensions similar to those previously reported for vesicular preparations (12, 13) (Fig. S1*B*). Using flow cytometry analysis of DiO-positive vesicles with counting beads, we estimated that we recovered 2.1×10^5 vesicles per milliliter of culture. Third, analysis of pelleted supernatant material by quasielastic light scattering (QELS) revealed two populations of particles of 200 to 300 nm, with a smaller population of 50 nm in diameter (Fig. S1*C*). The size distribution measured by QELS is larger than measured by electron microscopy, consistent with the fact that these techniques tend to overestimate and underestimate vesicular diameters, respectively (24). Fourth, a pulse-chase experiment with *B. anthracis* Sterne cells labeled with C^{14}-glycerol revealed the rapid accumulation of radioactivity in structures that could be recovered from the supernatant by centrifugation (Fig. S1*D*). Nevertheless, we worried about the potential for artifactual findings, given that phospholipids are notoriously prone to forming lamellar/vesicular structures or that the putative vesicles were remains of dead cells. Consequently, we placed heat-killed bacteria in growth media, incubated them in culture conditions identical to that with live bacterial cells and attempted to isolate vesicles. Vesicles were not recovered from a suspension of dead bacteria. Lastly, ζ potential analysis of vesicle preparations from *B. anthracis* Sterne 34F2 (Tox^+) and DeltaT (Tox^-) strains revealed values of -65.67 ± 4.71 mV and -7.94 ± 4.71 mV, respectively ($P < 0.05$). The large difference in ζ potential for vesicles produced by toxin-producing and deficient *B. anthracis* strains strongly argues against a random assembly of phospholipids or cell membrane fragments into vesicles.

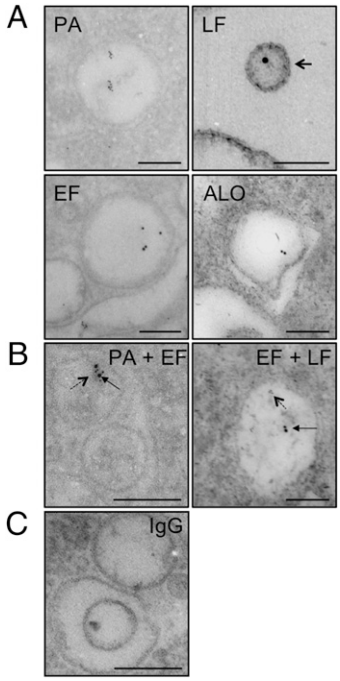

Fig. 1. (*A*) Immunogold localization of toxin components and anthrolysin in isolated vesicles. Immunoelectron microscopy with mAbs 7.5G (PA), BD3 (EF), 14FA (LF), and 64F8 (ALO) revealed gold particles in isolated vesicles. Arrow shows a vesicle with double membrane. (*B*) Immunogold double-labeling with mAbs 10F4 (PA), BD3 (EF), and 14FA (LF). Solid arrows, gold particles (10 nm) depicting EF binding; dashed arrows, gold particles (6 nm) depicting PA or LF binding. (*C*) Immunogold labeling with irrelevant IgG did not reveal gold particles in isolated vesicles. (Scale bars, 200 nm.)

***B. anthracis* Vesicles Contain Toxin Components.** The presence of toxin components in vesicles was initially characterized by ELISA. In this ELISA, polystyrene plates were coated with sonicated vesicle preparations and the reactivity of mAbs 7.5G IgG2a, 14FA IgG2b, and FF7 IgG1to PA, LF, and EF, respectively, was measured. Monoclonal Abs reacted with the vesicle preparation by ELISA with the relative reactivity of PA > LF > EF (Fig. S2*A*).

Effect of Vesicles on Murine Macrophages. Addition of vesicles to macrophage monolayers resulted in significant reduction in cell viability as measured by MTT cell viability assay (Fig. S2*B*). Vesicles from Sterne δ (Tox^-) strain also mediated cellular toxicity (Fig. S2*B*), a finding that we attributed to their anthrolysin (ALO) content. Bacterial cells that were separated from macrophages by 0.4-μm cell strainers mediated macrophage toxicity consistent with either vesicle-associated toxin diffusion or release of toxins from vesicles with subsequent diffusion across the barrier (Fig. S2*C*). Addition of neutralizing mAbs to isolated toxin components was previously shown to protect macrophage monolayers (25, 26). The addition of mAbs to vesicular preparations from Sterne 34F2 strain did not reduce toxicity to the macrophage monolayer (Fig. S2*D*). We surmised that the inability of the mAbs to protect against Sterne vesicles was a result of ALO-mediated toxicity. Hence, we isolated vesicles from Sterne ALO-null strain and repeated the vesicle toxicity experiments. When we added isolated vesicles to macrophage monolayers, we found that a neutralizing mAb to PA reduced vesicular toxicity (Fig. S2*E*).

Estimation of Free vs. Vesicle-Associated Toxin Amounts. To estimate the percentage of free toxin in culture supernatants, we used two assays: capture ELISA and MTT cell assay of centrifuged and noncentrifuged supernatant fractions. We centrifuged the supernatant to remove vesicles, concentrated, and measured PA concentration by capture ELISA, as described (25, 27). No soluble toxin was detected by capture ELISA in concentrated supernatants. In contrast, immunoblot analysis of the sedimentable fraction (vesicles) was positive for PA and EF (Fig. S2*F*). Addition of centrifuged concentrated supernatant (vesicle-free) to macrophage monolayers had no effect in cell viability (Fig. S2*D*), suggesting that there was little soluble toxin. In contrast, all of the cytotoxic activity was associated with the sedimentable fraction (Fig. S2*G*). Hence, the majority of the toxin appears to be vesicle-associated.

Immunogold Electron Microscopy of mAb Binding to Vesicles. Immunogold electron microscopy (IEM) of purified vesicles using mAbs to toxin components revealed gold particles within vesicles (Fig. 1*A*). We also demonstrated the presence of ALO in purified vesicles (Fig. 1*A*). To determine if vesicles transported one or more toxin components, we performed double-labeling IEM using mAbs to two toxin components simultaneously and discriminating each toxin with secondary IgG-specific mAbs labeled with gold particles of different sizes. IEM revealed gold particles representing the presence of PA and EF in the same vesicle, as well as EF and LF in the same vesicle (Fig. 1*B*). IEM of *B. anthracis*-germinated cells revealed the presence of vesicles with gold particles representing toxin components within bacterial cells (Fig. 2 *A*–*C*). IEM with isotype-matched, irrelevant mAbs revealed was negative for gold deposition (Figs. 3*C* and 4*D*). To explore the location of toxin components in the vesicles, we counted the proportion of gold particles in the lumen and on the surface of vesicles. The ratio of gold particles in the lumen to

MICROBIOLOGY

surface was 6.5: 1 (n = 323 gold particles), suggesting that toxin was primarily in the intravesicular compartment. In addition, high resolution IEM of bacterial cells revealed concentrations of gold particles at or near the bacterial surface, suggesting the vesicles emerged from the cell membranes (Fig. 2 *E* and *F*). Imaging of *B. anthracis*-infected macrophages revealed vesicle-like structures that stained for anthrax toxin by IEM were apparent in close proximity to macrophage membranes (Fig. 3*A*). Vesicle-like structures that stained for anthrax toxin by IEM were apparent inside macrophage cells containing *B. anthracis* (Fig. 3*B*).

Immunization of Mice with Purified Vesicles and Survival Studies. Unsonicated vesicles were immunogenic in BALB/c mice. Mice produced serum antibody responses to purified toxins by 6 wk after the initial immunization with immune serum reacting to rPA, rLF, and rEF by ELISA (Fig. 4*A*). Vesicle-associated proteins were separated by SDS/PAGE, incubated with pooled sera from immunized mice, and antibody binding was shown by immunoblot. Vesicle-associated proteins are recognized by sera from immunized mice (Fig. 4*A*, *Inset*). Interestingly, mice immunized with vesicles produced more IgM than IgG (Fig. 4*B*) but immunization with purified toxins produces primarily IgG (26, 27). We then evaluated the ability of unsonicated vesicles to elicit protective immunity by challenging vesicle-immunized mice with *B. anthracis* Sterne strain. Survival of vesicle-immunized mice was significantly prolonged compared with control mice immunized with adjuvant alone, with a median survival of 13 and 2 d, respectively ($P < 0.05$) (Fig. 4*C*).

Proteomic Analysis of Vesicles and *B. anthracis*. Thirty-six different proteins involved in a number of bacterial cellular processes were identified in purified vesicles (Fig. S3). These processes ranged from protein, carbohydrate and amino acid metabolism to proteins involved in cell-wall architecture, such as an S-layer protein. In addition, several proteins involved in the stress response such as HSP60 were also identified. Analysis of the protein composition components of *B. anthracis* cells revealed 89 different proteins involved in several bacterial cellular processes with 11 proteins in common with purified vesicles (Fig. S3).

Fatty Acid Profile of Vesicles and *B. anthracis*. Twelve and 16 lipids were identified from *B. anthracis* Sterne 34F2 bacterial cells and purified vesicles, respectively (Table S1). Palmitic and stearic acids were the major fatty acids identified for both cells and vesicles, but there were considerable differences on the composition of the minor lipid components, with vesicles being enriched in myristic and palmitic acids (Table S1).

Discussion

We demonstrate the isolation of vesicles from culture supernatants of the pathogenic, Gram-positive bacterium, *B. anthracis*. This result confirms and extends reports of vesicular structures in other Gram-positive microbes, such as *S. aureus* (21), *M. ulcerans* (19), and in *Bacillus cereus* and *Bacillus subtillis* (18). However, by demonstrating that these structures serve as a vesicular transport system for anthrax toxins, we associate vesicle production with the delivery of virulence components, as has been shown to such Gram-negative pathogens as *Escherichia coli* (28, 29), *P. aeruginosa* (14, 17, 30), and *Helicobacter pylori* (31) and *Cryptococcus neoformans* (12, 13).

Vesicle release is a ubiquitous process that occurs during normal bacterial growth and has been extensively characterized in Gram-negative bacteria (32). When vesicles are released from Gram-negative bacteria, a portion of the bacterial periplasm is taken along with other bacterial components, including bacterial proteins and DNA (18, 33, 34). In fact, the release of vesicles by pathogenic, Gram-negative bacteria is widely recognized as a strategy to deliver noxious cargos and virulence factors to target host cells (16, 31, 35, 36). Gram-negative vesicles are described to be spherical and bilayered structures ranging in size from 50 to 250 nm in diameter. Similarly, our group observed *B. anthracis* vesicle structures of comparable size that are spherical with bilayered membranes and electron-dense luminal contents. Light scattering analysis revealed a heterogenous population of vesicle diameter that was consistent with the size predicted from electron microscopic studies, with the caveat that these techniques overestimate and underestimate vesicle diameters (24, 37). We note with interest that the dimensions of Gram-positive, Gram-negative, and fungal vesicles are similar, despite a very high likelihood that the mechanisms of vesicle production differ markedly among these phylogenetically, distant microbes, which differ in cell-wall architecture. These similarities might reflect physical constraints in the assembly of lipid vesicles.

We investigated the presence of toxin components in vesicles isolated from *B. anthracis* Sterne 34F2 using mAbs previously generated by our group to the bacterium's toxin components (22, 25, 26), as well as anthrolysin (ALO) (38). Immunogold labeling studies for PA, LF, and EF revealed gold particles predominantly

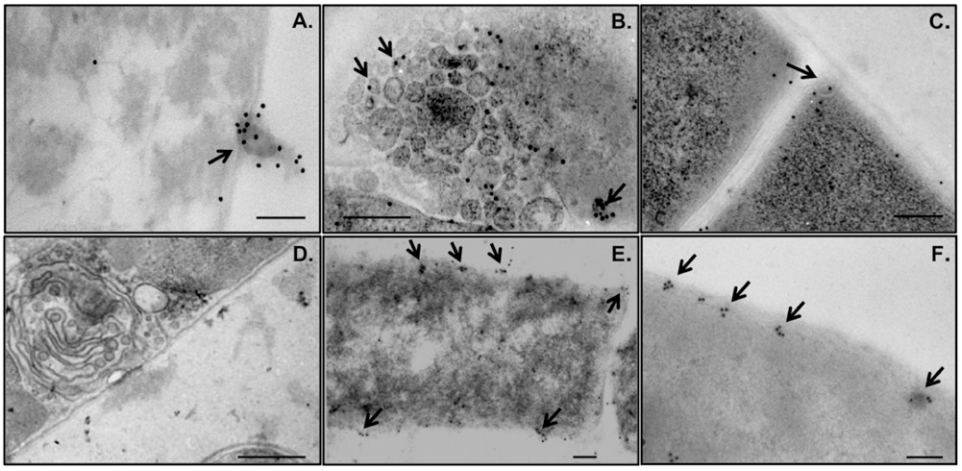

Fig. 2. Immunogold localization of PA, LF, and EF in *B. anthracis* Sterne 34F2. IEM with mAbs (*A*) FF7 (EF), (*B*) 10F4 (PA), and (*C*) 14FA (LF) revealed gold particles (solid arrows) in structures resembling vesicles. (*D*) Immunogold labeling with irrelevant IgG did not reveal gold particles in bacterial cells. (Scale bars, 200 nm.) (*E* and *F*) High-resolution IEM with mAb 7.5G (PA) of bacterial cells revealed concentrations of gold particles (solid arrows) at or near the bacterial surface. (Scale bars, 100 nm.)

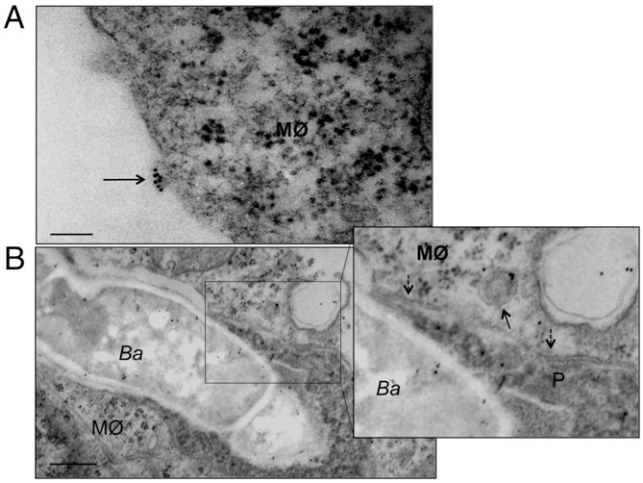

Fig. 3. Immunogold localization of macrophages incubated with *B. anthracis* with mAb 10F4. (*A*) Gold particles (10 nm) depicting PA in vesicle-like structure were detected bound to the surface of macrophages (arrow). (Scale bar, 100 nm.) (*B*) *B. anthracis* bacterial cells (*Ba*) are located within phagosomes (P) of macrophages (MØ). We note a disruption in phagosome double membrane (dashed arrow) and a vesicle containing PA (solid arrow) in the cytoplasm of the host cell in close proximity to an ingested bacterial cell. (Scale bar, 500 nm.)

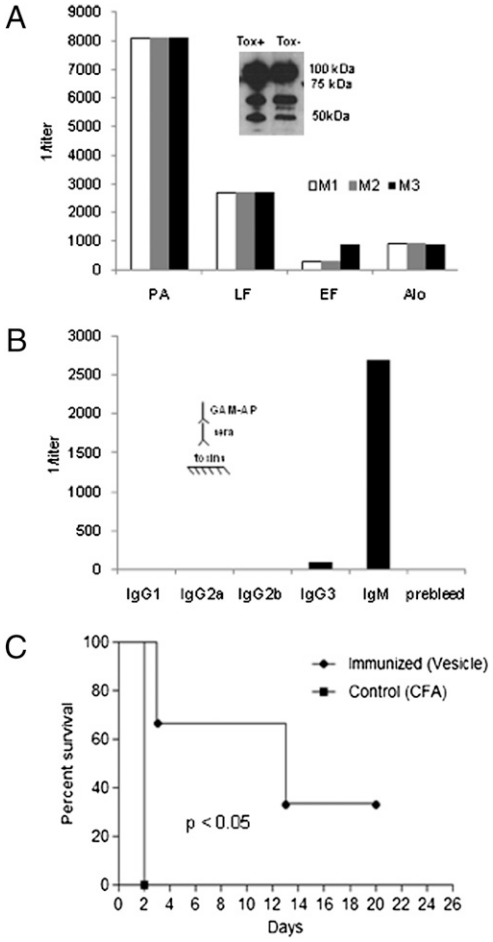

Fig. 4. Immunogenicity of isolated vesicles from *B. anthracis* Sterne 34F2 in mice. (*A*) Ab titer of BALB/c mice immunized with isolated vesicles as measured by ELISA. Mice (M1, M2, and M3) were immunized with vesicles. Inset, immunoblot of Tox^+ and Tox^- vesicles incubated with sera from vesicle-immunized mice. (*B*) Isotype analysis of immune sera from vesicle-immunized mice reveals a robust IgM response. (*Inset*) ELISA schematic which applies to *A* and *B*. (*C*) Survival of BALB/c mice immunized with isolated vesicles, mice immunized with adjuvant alone (control) and challenged with *B. anthracis* Sterne (Tox+) (10^6 cells i.v.). $n = 3$ each group.

in the lumen of isolated vesicles consistent with an intravesicular location. Immunoblot analysis confirmed the presence of toxin components in purified vesicles from *B. anthracis* Sterne. Furthermore, we determined the ζ potentials of isolated vesicles and determined that vesicles from the wild-type strain had a higher ζ potential than those from a toxin-deficient strain. Given that toxin proteins are negatively charged (pI: PA, 5.66; EF, 6.74; LF, 5.69) (http://ca.expasy.org/cgi-bin/pi_tool), we interpret this result as implying that toxin proteins contribute to the vesicle ζ potential.

B. anthracis vesicles represent potential potent vehicles for toxin transmission to host cells. Isolated vesicles mediated cellular toxicity in a fashion similar to recombinant LeTx, confirming their cytotoxic potential. Anthrax toxin is a tripartite toxin and by delivering the toxins in concentrated pockets, the bacteria could maximize their potency by packaging proteins that must interact together, and thus avoid the problem of protein dilution that would inevitably occur after diffusion from bacterial surfaces. To that end, IEM analysis revealed the presence of more than one toxin component in the same vesicle. We noted that PA-neutralizing antibody was ineffective in protecting macrophage monolayers against LeTx, a fact that we attribute to the presence of ALO, a potent cholesterol-dependent cytolysin that rapidly kills neutrophils and macrophages in vitro (39). In fact, vesicles from the toxin-deficient Sterne δT also mediated cellular toxicity, which we attribute to the presence of ALO. A mAb to PA was effective at protecting macrophage monolayers against vesicles from ALO-deficient Sterne. The mechanism of antibody-mediated protection against vesicle-delivered toxin is not clear, because one might expect that intralumenal toxin is not accessible to immunoglobulins. One possibility for antibody-mediated neutralization is that vesicles release toxin before interacting with the host cell. Alternatively, it is conceivable that the mechanism of antibody action is analogous to that described for intracellular neutralization of lysteriolysin (40). Toxin packaging in vesicles may contribute to the partial efficacy of antibody (26) and vaccines (25) in experimental anthrax.

Vesicle interactions with macrophages might be expected to deliver toxin in a manner distinct from soluble toxin, and could result in the internalization of other bacterial components, such as membrane proteins in the host cells. On the other hand, vesicle immunization was effective in protecting mice against challenge with *B. anthracis*, suggesting the possibility that vesicular preparations may be developed into effective vaccines.

Proteomic analysis of the vesicles revealed a complex protein composition that included molecular chaperones and proteins involved in cell wall architecture, protein, and carbohydrate metabolism. Electron microscopy revealed that the *B. anthracis* extracellular vesicles were not a uniform population, with some vesicles having high electron density content consistent with different forms of cargo. We recovered disproportionately few vesicles relative to the number of cells in suspension, which we attribute to inherent instability of vesicles and disruption during the isolation process. Lipid analysis of isolated vesicles revealed the presence of various fatty acids, which have been identified in other Gram-positive bacteria, such as *S. aureus* (41–43). The metabolic labeling experiment revealed a rapid rise in radiation-associated sedimentable material that was followed by a decrease and then a steady state phase. The kinetics of radiation incorporation and recovery were reproducible and are consistent with a dynamic vesicle population, which persists for only a limited time before disgorging their contents into the supernatant.

In summary, we demonstrate that *B. anthracis* produces toxin-laden vesicles that are toxic to macrophages, yet are capable of inducing a protective response in immunized mice. Our observations suggest the need to consider vesicle-mediated toxicity in the pathogenesis of anthrax and provide a unique system for studying of secretory pathways in pathogenic, Gram-positive bacteria.

Materials and Methods

***Bacillus anthracis* Strains.** *B. anthracis* Sterne strain 34F2 ($pXO1^+$, $pXO2^-$) was obtained from Alex Hoffmaster at the Center for Disease Control (Atlanta, GA). *B. anthracis* Sterne 34F2 δT ($pXO1^-$, $pXO2^-$) was obtained from Stephen Leppla at the National Institute of Allergy and Infectious Diseases (Bethesda, MD). *B. anthracis* Sterne 7702 UT231 (ALO-null) and rALO was obtained from Richard Rest at Drexel University College of Medicine (Philadelphia, PA). Bacterial cultures were grown from frozen stock in brain heart infusion broth (Difco) at 37 °C for 18 h with shaking. Recombinant PA, EF, and LF were obtained from Wadsworth Laboratories, New York State Department of Health.

Monoclonal Antibodies and Fluorescence Probes. Monoclonal Abs for PA (7.5G γ2b and 10F4 γ1) of *B. anthracis* have been described (22, 26). Monoclonal Ab 14FA γ2b is specific for LF of *B. anthracis* (22). Monoclonal Abs BD3 μ and FF7 γ1 are specific to EF (27). Monoclonal Abs 62F7 μ and 64F8 γ1 are specific for ALO of *B. anthracis* (38). DiO (5 μM) (3,3′-dioctadecyloxacarbocyanine perchlorate; Vybrant DiO cell labeling solution) (Invitrogen, Molecular Probes) was used to stain vesicles.

Vesicle Isolation and Staining. Vesicles were isolated by modification of the techniques we have described for the recovery of *C. neoformans* vesicles from culture supernatants (13, 23). *B. anthracis* cultures were centrifuged at 3,000 × *g* for 15 min at 4 °C, supernatants were collected and again centrifuged at 4,000 × *g* and 10,000 × *g* (4 °C) to remove cellular debris. The resulting supernatant was concentrated using an Amicon ultrafiltration system (100 kDa) and centrifuged, as described above. To collect vesicles, the resulting supernatant was centrifuged at 50,000 × *g* for 1 h at 4 °C, pellets were washed with sterile PBS twice, each time suspending and centrifuging at 50,000 × *g* for 1 h at 4 °C. For some experiments, vesicles were disrupted by sonication (Sonic dismembrator Model 100; Fisher Scientific). Purified vesicles were stained for 1 h with 5 μM DiO with Vybrant DiO cell labeling solution. Vesicles were then washed twice with PBS and centrifuged at 50,000 × *g* for 1 h at 4 °C and then analyzed with Becton Dickinson LSR II digital bench top flow cytometer (two-color, four-laser system) (BD Biosciences). To quantitate the number of vesicles, fluorescent counting beads were added at a known concentration (4.9×10^5) to DiO-stained purified vesicles before analysis (CountBright Absolute counting beads; Invitrogen). Data were analyzed with FlowJo software (Tree Star, Inc., Ashland, OR).

Measurement of Vesicle Size by QELS. The effective diameter and size distribution of vesicles preparations in 10 mM dextrose were measured using a 90Plus/BI-MAS Multi Angle Particle Sizing analyzer (Brookhaven Instruments Corp.), as described (37).

Pulse-Chase Labeling of *B. anthracis* with C^{14}-glycerol. *B. anthracis* cells (1:100 dilution of overnight culture) were grown in brain heart infusion media until OD 600 nm of 0.5. For pulse labeling, 0.4 μCi of C^{14}-glycerol (specific activity, 142.7 mCi/mmol; Perkin-Elmer) per milliliter of culture was added and incubated for 5 min. Labeled *B. anthracis* cultures were then centrifuged, suspended in unlabeled media, and cultured at 37 °C while shaking for several chase times. Vesicles were isolated as described above and incorporation of C^{14} was measured using 1450 Microbeta liquid scintillation reader (Perkin-Elmer Wallace, Inc.).

ζ Potential Measurements. The ζ potential of vesicles samples suspended in 10 mM dextrose were calculated in a ζ potential analyzer (ZetaPlus; Brookhaven Instruments Corp.) (44, 45).

ELISA. The presence of toxin components in vesicles was measured using ELISA, as previously described (25, 26, 46).

Western Blot Analysis. Isolated vesicles were solubilized in Laemmli sample buffer containing β-mercaptoethanol, boiled for 10 min, separated on a 12% SDS/PAGE, stained overnight with GelCode Blue Stain (Pierce), and visualized with ECL chemiluminescence kit (Pierce) (47). Membranes were incubated with either mAbs 10F4 IgG1 or BD3 IgM, as described (26, 27).

MTT Cell Assay. MTT [3, (4,5-dimethylthiazol-2-yl) 2,5-diphenyltetrazolium bromide] assay was used to determine toxicity of vesicles to J774 mouse macrophage cell line as described (25, 26). In some experiments, 0.4-μm cell strainers (Fisher Scientific) were used to separate bacterial cells from macrophages to ascertain the toxicity of secreted vesicles.

IEM. *B. anthracis* vesicles and germinated bacterial cells were fixed with 2.5% glutaraldehyde in 0.1 M phosphate buffer. For localization of vesicles associated with macrophages, bacterial cells (10^6) were incubated with a monolayer of J774 macrophages and fixed with 2.5% glutaraldehyde in 0.1 M phosphate buffer. IEM were then performed as described previously (22) with 10 μg of mAbs 7.5G (PA), 10F4 (PA), FF7 (EF), and 14FA (LF).

Protein Analysis of *B. anthracis* and Isolated Vesicles. Cellular and vesicular proteins were resolved as described above. For LC-MS/MS analysis, protein was digested and product were separated by a 60-min gradient elution at a flow rate of 0.250 μL/min equipped with the Dionex 3000 nano-HPLC system directly interfaced with the Thermo LTQ-Orbitrap mass spectrometer. DTA files generated by Bioworks 3.3.1 software (Thermo Scientific) were searched against the bacterial database using an in-house Mascot searching algorithm. The following search parameters were used in all of the Mascot searches: maximum of one missed trypsin cleavages, cysteine carbamidomethylation as fixed modification, and methionine oxidation as the variable modification. The maximum error tolerance is 10 ppm for MS and 1.2 Da for MS/MS.

Fatty Acid Analysis of Bacterial Cells and Isolated Vesicles. Bacterial cells and vesicles were dried under a stream of N_2, suspended in 200 μL of 1 N KOH in 75% ethanol and heated at 70 °C for 3 h. The reaction was acidified with 200 μL of 6 N HCl, followed by the addition of 20 mg of Na_2SO_4. Lipids were extracted with 400 μL of chloroform and dried with N_2. Saponified lipids were derivatized to fatty acids methyl esters by dissolving the extracted fatty acids in75 μL of the derivative methanolic-HCl (Sigma). The samples were incubated at 60 °C for 3 h, dried with N_2, suspended in 50 μL of hexane, and analyzed by GC/FID using an Agilent 7890 GC system equipped with a FID detector. A capillary column BPS-70 (30 m × 0.25 mm × 0.25 μm) was used and 1 μL of sample was injected with a split ratio of 25:1 and a helium flow of 1.2 mL/min. The inlet temperature was held at 225 °C and the temperature program was 120 °C initial, increased by 15 °C/min to 170 °C, then increased by 5 °C/min to 225 °C and held for 3 min. Each fatty acids methyl ester was determined by its retention time compared with the standard mix run in the same chromatographic sequence.

Animal Studies. Female BALB/c mice (6–8 wk) (National Cancer Institute) were immunized intraperitoneally with isolated unsonicated vesicles in complete Freund's adjuvant (CFA) (Sigma). Two weeks later, the mice were boosted with isolated vesicles in incomplete Freund's adjuvant. Mice were bled from the retroorbital sinus, sera was collected and stored at −20 °C for later analysis of Ab titers by ELISA. For survival experiments, vesicle-immunized BALB/c mice or CFA-immunized (control) were infected i.v. with 10^6 cells of *B. anthracis* strain Sterne 34F2. Mice were monitored daily for mortality. All animal work was done in accordance with regulations of the Institute for Animal Studies at the Albert Einstein College of Medicine.

Statistical Analysis. Statistical analyses for light scattering and ζ potential experiments were done with 90 Plus/BI-MAS Software (Brookhaven Instruments Corp.). Survival data were analyzed by log rank analysis ($P < 0.05$) (Sigmastat).

ACKNOWLEDGMENTS. We thank Dr. Allan Guimarães for his help with proteomics analysis, Geoff Perumal and Leslie Gunther from the Analytical Imaging Facility at the Albert Einstein College of Medicine (AECOM) for help with EM, Dr. HaiTeng Deng and Dr. Joseph Fernandez from the Proteomics facility at The Rockefeller University for analyzing the protein composition, and Dr. Gustavo Palacios of Stable Isotope and Metabolomics Core of AECOM for analyzing the fatty acid profiles. This work was supported in part by the Northeastern Biodefense Center under Grant U54-AI057158-Lipkin. A.C. is supported by Grants AI33774-11, HL59842-07, AI33142-11, and AI52733-02. R.J.B.C. is supported by the Training Program in Cellular and Molecular Biology and Genetics (T32 GM007491).

1. Inglesby TV, et al.; Working Group on Civilian Biodefense (1999) Anthrax as a biological weapon: Medical and public health management. *JAMA* 281:1735–1745.
2. Inglesby TV, et al.; Working Group on Civilian Biodefense (2002) Anthrax as a biological weapon, 2002: Updated recommendations for management. *JAMA* 287: 2236–2252.
3. Mock M, Fouet A (2001) Anthrax. *Annu Rev Microbiol* 55:647–671.
4. Collier RJ, Young JA (2003) Anthrax toxin. *Annu Rev Cell Dev Biol* 19:45–70.
5. Mock M, Mignot T (2003) Anthrax toxins and the host: A story of intimacy. *Cell Microbiol* 5(1):15–23.
6. Kintzer AF, et al. (2010) Role of the protective antigen octamer in the molecular mechanism of anthrax lethal toxin stabilization in plasma. *J Mol Biol* 399:741–758.
7. Kintzer AF, et al. (2009) The protective antigen component of anthrax toxin forms functional octameric complexes. *J Mol Biol* 392:614–629.
8. Leppla SH (1982) Anthrax toxin edema factor: A bacterial adenylate cyclase that increases cyclic AMP concentrations of eukaryotic cells. *Proc Natl Acad Sci USA* 79: 3162–3166.
9. Leppla SH (1984) *Bacillus anthracis* calmodulin-dependent adenylate cyclase: Chemical and enzymatic properties and interactions with eucaryotic cells. *Adv Cyclic Nucleotide Protein Phosphorylation Res* 17:189–198.
10. Ellis TN, Kuehn MJ (2010) Virulence and immunomodulatory roles of bacterial outer membrane vesicles. *Microbiol Mol Biol Rev* 74(1):81–94.
11. Kuehn MJ, Kesty NC (2005) Bacterial outer membrane vesicles and the host-pathogen interaction. *Genes Dev* 19:2645–2655.
12. Rodrigues ML, et al. (2008) Extracellular vesicles produced by *Cryptococcus neoformans* contain protein components associated with virulence. *Eukaryot Cell* 7(1):58–67.
13. Rodrigues ML, et al. (2007) Vesicular polysaccharide export in *Cryptococcus neoformans* is a eukaryotic solution to the problem of fungal trans-cell wall transport. *Eukaryot Cell* 6(1):48–59.
14. Kadurugamuwa JL, Beveridge TJ (1995) Virulence factors are released from *Pseudomonas aeruginosa* in association with membrane vesicles during normal growth and exposure to gentamicin: A novel mechanism of enzyme secretion. *J Bacteriol* 177: 3998–4008.
15. Kadurugamuwa JL, Beveridge TJ (1996) Bacteriolytic effect of membrane vesicles from *Pseudomonas aeruginosa* on other bacteria including pathogens: Conceptually new antibiotics. *J Bacteriol* 178:2767–2774.
16. Kadurugamuwa JL, Beveridge TJ (1999) Membrane vesicles derived from *Pseudomonas aeruginosa* and *Shigella flexneri* can be integrated into the surfaces of other Gram-negative bacteria. *Microbiology* 145:2051–2060.
17. Bauman SJ, Kuehn MJ (2009) *Pseudomonas aeruginosa* vesicles associate with and are internalized by human lung epithelial cells. *BMC Microbiol* 9:26.
18. Dorward DW, Garon CF (1990) DNA is packaged within membrane-derived vesicles of Gram-negative but not Gram-positive bacteria. *Appl Environ Microbiol* 56:1960–1962.
19. Marsollier L, et al. (2007) Impact of *Mycobacterium ulcerans* biofilm on transmissibility to ecological niches and Buruli ulcer pathogenesis. *PLoS Pathog* 3(5):e62.
20. Lee EY, et al. (2009) Gram-positive bacteria produce membrane vesicles: Proteomics-based characterization of *Staphylococcus aureus*-derived membrane vesicles. *Proteomics* 9:5425–5436.
21. Kim SH, et al. (2009) Structural modifications of outer membrane vesicles to refine them as vaccine delivery vehicles. *Biochim Biophys Acta* 1788:2150–2159.
22. Rivera J, et al. (2009) Radiolabeled antibodies to *Bacillus anthracis* toxins are bactericidal and partially therapeutic in experimental murine anthrax. *Antimicrob Agents Chemother* 53:4860–4868.
23. Casadevall A, Nosanchuk JD, Williamson P, Rodrigues ML (2009) Vesicular transport across the fungal cell wall. *Trends Microbiol* 17(4):158–162.
24. Egelhaaf SU, Wehrli E, Muller M, Adrian M, Schurtenberger P (1996) Determination of the size distribution of lecithin liposomes: A comparative study using freeze fracture, cryoelectron microscopy, and dynamic light scattering. *J Microsc* 184:214–228.
25. Abboud N, et al. (2009) Identification of linear epitopes in *Bacillus anthracis* protective antigen bound by neutralizing antibodies. *J Biol Chem* 284:25077–25086.
26. Rivera J, et al. (2006) A monoclonal antibody to *Bacillus anthracis* protective antigen defines a neutralizing epitope in domain 1. *Infect Immun* 74:4149–4156.
27. Winterroth L, Rivera J, Nakouzi AS, Dadachova E, Casadevall A (2010) Neutralizing monoclonal antibody to edema toxin and its effect on murine anthrax. *Infect Immun* 78:2890–2898.
28. Kesty NC, Kuehn MJ (2004) Incorporation of heterologous outer membrane and periplasmic proteins into *Escherichia coli* outer membrane vesicles. *J Biol Chem* 279: 2069–2076.
29. Kesty NC, Mason KM, Reedy M, Miller SE, Kuehn MJ (2004) Enterotoxigenic *Escherichia coli* vesicles target toxin delivery into mammalian cells. *EMBO J* 23: 4538–4549.
30. Bauman SJ, Kuehn MJ (2006) Purification of outer membrane vesicles from *Pseudomonas aeruginosa* and their activation of an IL-8 response. *Microbes Infect* 8:2400–2408.
31. Fiocca R, et al. (1999) Release of *Helicobacter pylori* vacuolating cytotoxin by both a specific secretion pathway and budding of outer membrane vesicles. Uptake of released toxin and vesicles by gastric epithelium. *J Pathol* 188:220–226.
32. Beveridge TJ (1999) Structures of Gram-negative cell walls and their derived membrane vesicles. *J Bacteriol* 181:4725–4733.
33. Dorward DW, Garon CF, Judd RC (1989) Export and intercellular transfer of DNA via membrane blebs of *Neisseria gonorrhoeae*. *J Bacteriol* 171:2499–2505.
34. Kolling GL, Matthews KR (1999) Export of virulence genes and Shiga toxin by membrane vesicles of *Escherichia coli* O157:H7. *Appl Environ Microbiol* 65:1843–1848.
35. Kadurugamuwa JL, Beveridge TJ (1998) Delivery of the non-membrane-permeative antibiotic gentamicin into mammalian cells by using *Shigella flexneri* membrane vesicles. *Antimicrob Agents Chemother* 42:1476–1483.
36. Li Z, Clarke AJ, Beveridge TJ (1998) Gram-negative bacteria produce membrane vesicles which are capable of killing other bacteria. *J Bacteriol* 180:5478–5483.
37. Eisenman HC, Frases S, Nicola AM, Rodrigues ML, Casadevall A (2009) Vesicle-associated melanization in *Cryptococcus neoformans*. *Microbiology* 155:3860–3867.
38. Nakouzi A, Rivera J, Rest RF, Casadevall A (2008) Passive administration of monoclonal antibodies to anthrolysin O prolong survival in mice lethally infected with *Bacillus anthracis*. *BMC Microbiol* 8:159.
39. Mosser EM, Rest RF (2006) The *Bacillus anthracis* cholesterol-dependent cytolysin, Anthrolysin O, kills human neutrophils, monocytes and macrophages. *BMC Microbiol* 6:56.
40. Edelson BT, Unanue ER (2001) Intracellular antibody neutralizes Listeria growth. *Immunity* 14:503–512.
41. Lambert MA, Moss CW (1976) Cellular fatty acid composition of *Streptococcus mutans* and related streptococci. *J Dent Res* 55:A96–A102.
42. Nair MK, et al. (2005) Antibacterial effect of caprylic acid and monocaprylin on major bacterial mastitis pathogens. *J Dairy Sci* 88:3488–3495.
43. Sado-Kamdem SL, Vannini L, Guerzoni ME (2009) Effect of alpha-linolenic, capric and lauric acid on the fatty acid biosynthesis in *Staphylococcus aureus*. *Int J Food Microbiol* 129:288–294.
44. Fonseca FL, et al. (2010) Immunomodulatory effects of serotype B glucuronoxylomannan from *Cryptococcus gattii* correlate with polysaccharide diameter. *Infect Immun* 78:3861–3870.
45. Frases S, Nimrichter L, Viana NB, Nakouzi A, Casadevall A (2008) *Cryptococcus neoformans* capsular polysaccharide and exopolysaccharide fractions manifest physical, chemical, and antigenic differences. *Eukaryot Cell* 7:319–327.
46. Casadevall A, Mukherjee J, Scharff MD (1992) Monoclonal antibody based ELISAs for cryptococcal polysaccharide. *J Immunol Methods* 154(1):27–35.
47. Laemmli UK (1970) Cleavage of structural proteins during the assembly of the head of bacteriophage T4. *Nature* 227:680–685.